

Charring Rate of Wood for ASTM E 119 Exposure

Robert H. White* and Erik V. Nordheim**

Abstract

Analytical methods that predict the endurance of structural wood members in a fire are based on the reduction of the cross section of the member caused by wood being charred. To define the charring rate in terms of more fundamental properties, empirical models were established. Eight species were tested for charring rates and material properties. Regression analysis was used to develop the models. The predictor variables for the initial factorial design included density, moisture content, treatability, and hardwood-softwood classification. The addition of char contraction simplified the model and reduced the predictor variables to the char contraction factor, density, and moisture content. Our results show the importance of surface recession and moisture content to wood charring.

Introduction

Building code requirements for fire-rated assemblies have constrained the competitiveness of wood construction in nonresidential markets. The fire resistance rating of an assembly is usually experimentally determined in accordance with the American Society for Testing and Materials (ASTM) standard test method E 119.¹ This ASTM test method is expensive to use, and analytical methods for determining the fire resistance rating of a wood assembly are an inexpensive alternative. Analytical methods have been

*Research Wood Scientist, USDA Forest Service, Forest Products Laboratory, One Gifford Pinchot Drive, Madison, WI 53705-2398

**Professor of Forest and Statistics, Forest Department, University of Wisconsin-Madison, 120 Russell Laboratories, Madison, WI 53706

The Forest Products Laboratory is maintained in cooperation with the University of Wisconsin. This article was written and prepared by U.S. Government employees on official time, and it is therefore in the public domain and not subject to copyright.

Keywords: Wood, charring, regression analysis, empirical models

developed for predicting the fire resistance of heavy timber members and wooden light-frame assemblies.² These analytical methods are based on the reduction of the cross section of the member caused by the wood being charred and the subsequent loss in the strength of the member. Available data have shown that the charring rate of wood in the standard ASTM E 119 test¹ is a function of the species, density, and moisture content. Many different species of wood exist; therefore, models are needed to explain the species difference in terms of more fundamental properties.

The overall objective of this work was to understand the important factors affecting the variability in fire performance of different wood species. The specific objective was to develop empirical models that predict the species difference in charring rates in terms of basic wood characteristics and that are applicable for all species.

Literature Review

Wood undergoes thermal degradation when exposed to fire. Thermal degradation or pyrolysis reduces the density by changing the wood to char and gases. Glowing combustion and mechanical disintegration will eventually ablate the outer char layer. The pyrolysis gases undergo flaming combustion as they leave the charred wood surface. The pyrolysis, charring, and combustion of wood have been extensively studied.³⁻⁷

Charring Rate

The charring rate of wood generally refers to the dimensional rate, such as millimeters per minute, at which wood changes to char. Many factors are involved in wood charring. Kanury and Blackshear⁸ examined various physiochemical effects, including diffusion of condensable vapors inward, internal convection outward, properties of the partially charred wood, kinetics of pyrolysis, energetic of pyrolysis, and postdecomposition reactions. Wood charring factors mentioned by Lee and others⁹ included external heating rate, total time of heating, and anisotropic properties of wood and char relative to the internal flow of heat and gas.

Different Species

Several studies have been conducted on the charring rates of different wood species. Bryan and Doman¹⁰ reported the comparative fire resistance of 85 British and other species. McNaughton¹¹ reported fire resistance results for 17 North American species. In tests on eight species, Thomas and others¹² found the rate of weight loss increased with the intensity of radiation, the density, and the actual or effective permeability. Schaffer¹³ reported charring rates for white oak, Douglas fir, and southern pine. In tests of laminated wood columns with a 15-percent moisture content (MC)

level, the charring rate of western hemlock perpendicular to the plane of the lamination was 16 percent slower than that for Douglas fir and 28 percent slower than red cedar and Scots pine heartwood (European redwood).¹⁴

Wood Characteristics

Various characteristics of wood affect the charring rate. Some characteristics are density moisture content, permeability, anatomy, and chemical composition. Density is recognized as the major factor in charring rates. Schaffer¹³ found that denser wood had a slower charring rate. Hall and others¹⁵ also obtained a similar relationship between density and charring in tests of 13 hardwood and 2 softwood species.

The moisture content level also was a significant factor in the regression equations of Schaffer.¹³ Williams¹⁶ considered moisture to have three effects on the fire performance of wood: changes in the thermal properties, the heat of wetting, and the latent heat of moisture vaporization. In fire tests of glued laminated beams, Dorn and Egner¹⁷ found that the outer zones of the beam almost completely dried out but the moisture content level had increased 2 to 4 percent in the zones closer to the interior. White and Schaffer¹⁸ found that the fraction of initial moisture content driven into or generated within the wood slab depended upon the total initial moisture content level, the severity of the fire exposure, and the species.

Permeability may be a controlling factor in the movement of moisture. Tinney¹⁹ and Roberts²⁰ measured the pressure in heated wood cylinders and reported pressure drops when structural changes were observed. Kanury and Blackshear,⁸ in their discussion of secondary processes affecting wood burning, stressed the importance of internal convection as a result of outflow of pyrolysis gases. Fredlund⁴ measured internal pressures as a function of time while subjecting wood to a fixed radiant flux, and included permeability in his theoretical model.

Another explanation for the species factor in wood charring is chemical composition, which influences kinetics and energetic of pyrolysis. As described by Tang,²¹ the less-stable minor wood components begin to decompose at 150°C to 200°C, and the major components decompose at temperatures up to 500°C. The cellulose fraction contributes most to flaming combustion, and the lignin fraction supports most of the subsequent glowing combustion. Under a scanning electron microscope, Knudson and Williamson²² viewed Douglas fir that had been pyrolyzed up to 30 min at 250°C, 350°C, and 550°C. They concluded that the various cell wall components had decomposed at rates related to their chemical composition. Based on tests of five species by Thomas and others,¹² Hadvig and Paulsen²³ obtained a correlation between the incident thermal radiation required for mass loss and the ratio of lignin to hemicellulose.

A final factor that affects the charring rate is the anatomical characteristic of the wood. Lee and others⁹ noted that the anisotropic nature of wood can have a significant effect on the heat of reaction as a result of directional differences in the thermal conductivity and gas permeability of the wood and char.

Char Layer

The char layer and its fissures are important factors in wood charring. As a result of surface recession, the layer being charred is thinner than the original thickness of the wood that has charred. The thinner insulative char layer is important in the modeling of wood charring.²⁴ This surface recession can be due to chemical oxidation or mechanical degradation at the surface or contraction of the char. As noted by Roberts,²⁵ the fissures facilitate flow of volatile products and diminish the contact between the gases and the solid.

Experiments

In this work, we assumed the charring rate was a function of density, moisture content, transport properties, and chemical properties. Samples of eight different species were tested for charring rates and for several material properties such as chemical composition, permeability, and density

Experimental Design

To maximize the relative effects of density, permeability, and chemical composition in the regression analysis, the eight species to be tested were selected on the basis of a 2^3 factorial design.²⁶ The three variables in the design were density (low or high), permeability (low or high), and species type (hardwood or softwood). Although variability in wood properties and availability of materials prevented a true factorial design, the selection of materials provided the desired range of material properties.

The eight species tested were Engelmann spruce (*Picea engelmannii*), western red cedar (*Thuja plicata*), southern pine (*Pinus* sp.), redwood (*Sequoia sempervirens*), hard maple (*Acer* sp.), yellow-poplar (*Liriodendron tulipifera*), red oak (*Quercus* sp.), and basswood (*Tilia* sp.). Except for the 38-mm-thick (nominal 2- by 10-in.) southern pine, the 50-mm-thick (8/4 lumber) boards were relatively clear wood.

Methodology of Charring Tests

We tested the wood slabs in a small vertical gas-fired furnace. Forty charring tests were done in two groups. In the first group of 24 tests, three specimens from one board of each of the eight species were tested at moisture content levels of 6, 9, and 11 percent. In the subsequent group of 16 tests, two specimens from a second board of each of the eight species were

tested at moisture content levels of 9 and 16 percent. The 9 percent MC level corresponded to the conditioning specified in ASTM E 119.¹

For the purpose of preparing specimens, we assumed the properties were constant along the length of the 3-m boards. The 250-mm-wide boards were cut lengthwise into 63-mm-wide pieces. The materials for any one charring test and the corresponding material property tests came from the same 63-mm-wide piece. Except for southern pine, the 230-mm-high slabs consisted of five 46-mm-thick laminates glued together with phenol-resorcinol glue. The southern pine slabs consisted of seven 38-mm-thick laminates. The overall dimensions of the slabs were 230 mm high, 510 mm wide, and 63 mm thick.

Temperature measurements were taken in the middle three laminates. Within each laminate, two thermocouples were placed at each of four distances from the fire-exposed surface (13, 25, 38, and 51 mm), thus we had two replicates for each location. For each specimen, three sets of data were produced—one for each laminate. All three laminates came from the same board. The 30-gage (0.255-mm-diameter) iron-constantan thermocouple wires were laid across the top of the laminates with the ends placed in holes that had been drilled in the top of the laminates.

The refractory concrete furnace was equipped with pipe outlets for discharging natural gas into the interior of the furnace. The slabs were placed between two concrete blocks in the 515-mm-square opening on one side of the furnace. The temperature inside the furnace was recorded with a thermocouple in an iron-capped pipe 51 mm from the original surface of the slab. The input of natural gas into the furnace was regulated to control the temperature inside the furnace so that it followed the standard ASTM E 119 time-temperature curve. Air for combustion was admitted by natural draft through vents at the bottom of the furnace.

The tests were terminated when the last of the six thermocouples placed at a depth of 38 mm from the fire-exposed surface recorded 288°C (550°F), which is widely accepted as a criterion for the base of the char layer. As a result, the thermocouples at 51 mm from the fire-exposed surface were not included in the analysis of the data. The intent was to have data that are consistent with a semi-infinite slab. Specimens were weighed before the test, after reconditioning of the charred specimen, and weighed again after the char was scraped off. The charred specimens were also cut in half to obtain the thickness of the charred slab and the char layer.

The times to reach 288°C at the three fixed distances (13, 25, and 38 mm) from the original fire-exposed surface of the slab were analyzed from the charring tests. Within a given slab, six thermocouples (two for each of the three laminates) were placed at a given distance from the surface. The consistency of the times for the six thermocouples was reasonably good. The coefficients of variation for the six observations ranged from 1.4 to 13.6 percent.

Characteristics measured on the slabs included density, moisture content, orientation of the annual rings to the fire-exposed surface, and char contraction. The annual ring orientation was the angle of the annual rings from the fire-exposed surface of the laminates. For example, annual rings at a 90° angle ran in the direction of the charring. The char contraction factor was the thickness of the char layer at the end of the test divided by the char depth. The char depth was based on the original thickness of the wood member.

Supplementary Tests

Supplementary tests were conducted to determine material properties of the wood used in the charring tests. The three general groups of these properties were density and moisture content, transport properties, and chemical properties. These supplemental tests and the results obtained in this study are described in detail by White.⁷

The transport properties included longitudinal gas permeability, treatability, and diffusion coefficients. Transport properties were measured for the individual 63-mm-wide sections that were used to construct the slabs for the charring tests. Permeability measurements in the longitudinal direction (parallel to the direction of the wood fibers) are high enough that they are fairly easy to measure in a reliable manner. In these tests, the permeability transverse to the grain direction is likely to be the critical factor. However, permeability measurements transverse to the grain direction are very low and tend to be unreliable. As a result, we used treatability measurements as an indicator of the transverse permeability. Treatability properties were the depth of penetration and retention of a chemical when wood is pressure treated with the chemical. Treatability specimens were treated with copper chrome arsenate (CCA) preservative. A Chrome Azurol S and acetate solution was used to clearly delineate the treated zone. Longitudinal permeability was measured as a secondary indicator of the relative permeability of the boards. Permeability reflects the movement of fluids as a result of a pressure gradient. Movement of fluids may also be due to a concentration gradient. Resorption diffusion coefficients were measured as a relative indicator of moisture movement as a result of a concentration gradient.

The chemical properties included chemical composition, heat of combustion, and chemical kinetic parameters obtained by thermal gravimetric analysis (TGA). Chemical properties were determined for samples taken from the entire board rather than the individual 63-mm-wide sections. Thermal gravimetric analysis results provided a direct measurement of thermal degradation of a very small ground sample. Heats of combustion of ground wood and extractive-free wood were determined with an automatic adiabatic calorimeter and oxygen bomb. Heat of combustion results

provided an overall indicator of the combustion process. In the TGA, 5 to 10 mg of ground wood and extractive-free wood samples were heated in nitrogen from 25°C to 450°C at a rate of 10°C per minute. The activation energies and pre-exponential factors of the Arrhenius thermal degradation equation were calculated.

The chemical composition tests included ethanol-benzene extraction, sulfuric acid hydrolysis to obtain Klason lignin, high-performance liquid chromatography to obtain the five wood sugar monomers, treatment with sulfuric acid to obtain uronic anhydride, gas chromatography to obtain acetyl content, and dry ignition at 575°C to obtain the ash content. The percentages of cellulose and hemicellulose were calculated from the values for the five sugars, acetyl and uronic anhydride.

Model Development

As noted previously, the times to reach 288°C at distances (13, 25, and 38 mm) from the original fire-exposed surface of the slab were the data considered from the charring tests. The next step was to convert these data to values for charring rate. But first, we needed to establish the proper model or equation relating the char depth to the time or duration of the fire exposure. When we had a proper time-location model, we then developed a predictive model for the “char rate” parameter based on the material properties of the slab.

Time-Location Models

For each of the 40 slabs, the times for the thermocouple to reach 288°C were used to evaluate various models for the relationships between time and location of the char base. Four models for the relationship between time t and the distance of the char base from the original fire-exposed surface (x_c) were considered. The models were as follows:

$$t = mx_c \quad (1)$$

$$t = mx_c - b \quad (2)$$

$$t = mx_c^a \quad (3)$$

or the linear form of Equation (3)

$$\ln t = \ln m + a \ln x_c \quad (4)$$

and

$$t = dx_c + gx_c^2 \quad (5)$$

where m (reciprocal char rate) and a , b , d , and g (general parameters with no specific interpretation) were parameters to be estimated from empirical data t and x_c . The models developed in this section had time to reach the 288°C criterion (t) as the dependent variable and the distance from the original fire-exposed surface (x_c) i.e., char depth, as the independent variable. This was consistent with the experimental procedure in

which times of the 288°C criterion were recorded for the fixed thermocouple locations.

Equation (1) represents the way that char rate data are commonly used. This assumes time is linearly related to char depth. It is often assumed that it takes 40 min to reach a char depth of 25.4 mm (1 in.). Since no char layer is present at the start of the test, it is reasonable to assume that char rate is faster initially. Faster initial char rate and linear steady-state char rate can be represented by Equation (2). This equation is only valid when the linear steady-state char rate has been obtained. The parameter b accounts for the faster initial char rate. It is assumed in Equation (1) that the delay in the ignition of the surface negates the faster initial char rate. A progressively thicker insulated char layer would be expected to slow down the char rate with time. For steadily slower char rates, Equation (3) and Equation (5) are possible models. These equations also are possible models for steadily faster char rates. Equation (3) is a nonlinear model of the type that was used by Lawson and others²⁷ and Vorreiter.²⁸ Equation (3) allows for a nonlinear relationship between time and char depth. The parameter describes the relationship. If $\alpha < 1$, the model indicates times increasing more slowly with increase char depth; if $\alpha > 1$, times increase more quickly. When $\alpha = 1$, Equation (3) reduces to Equation (1). Equation (4) is a linear form of Equation (3). Equation (5), a model suggested by Kanury and Holve²⁹ for panels, adds a quadratic term to Equation (1). Linear regressions of the time compared to the location data for 13, 25, and 38 mm thermocouple locations provided estimates of the parameters in the equations.

Detailed analyses were performed on one slab from each of the eight species. This slab was randomly selected from the two slabs conditioned to 9 percent MC (23°C, 50percent relative humidity). All results reported here are from these eight slabs. Further analysis showed that the slabs were representative and the conclusions would not be altered in any important way if all slabs per species had been used.

We performed extensive analysis on data for the selected boards using Equations (1), (2), (4), and (5). We describe the methodology using Equation (2) (Table 1) and then summarize the results for all the equations.

The first issue to consider was whether the same parameter estimates of m and b were obtained for each of the three laminates of a slab (height effect) or whether different estimates are obtained. To examine this issue, we first considered the following "full model":

$$t_{ijk} = m_i x_{ijk} - b_i + e_{ijk} \quad (6)$$

In the full model, $i = 1, 2, 3$ indexes the top, middle, and bottom laminate; $j = 1, 2, 3$ indexes the 13-, 25-, and 38-mm depths within a laminate; and $k = 1, 2$ indexes the replicate thermocouple location within each laminate-depth combination; e_{ijk} represents the random error term. This full model

Table 1: Evaluation of Equation (2)

Model ^a	Item	Test number							
		3	20	22	32	33 ^b	35	39 ^b	43
Full	Lack of fit								
	F(3,9)	7.08	6.27	1.69	15.43	5.27	3.66	2.04	1.33
Reduced	Coefficient of determination (R^2)	0.995	0.991	0.984	0.991	0.994	0.977	0.985	0.986
	Coefficient of determination (R^2)	0.990	0.984	0.978	0.989	0.986	0.969	0.984	0.966
	Coefficient of variation	5.2	7.0	7.9	5.4	5.9	9.4	6.7	9.4
	m								
	Estimate	1.978	1.610	1.378	1.550	1.670	1.687	1.884	1.294
	Standard error	0.050	0.051	0.052	0.042	0.051	0.076	0.063	0.060
	b								
	Estimate	8.150	9.357	6.633	5.643	8.136	7.826	7.214	5.001
	Standard error	1.381	1.393	1.409	1.136	1.417	2.063	1.723	1.654
	Reduced model F value	3.08	2.32	1.07	0.90	3.30	1.04	0.27	4.27

^a The full model includes the effect of the different laminates on the results, whereas the reduced model is a single equation for the entire slab that does not include laminate location.

^b One pair of data missing in these tests.

allows for different values for m and b for each laminate. We then considered the following "reduced model":

$$t_{ijk} = mx_{ijk} - b + e_{ijk} \quad (7)$$

Equation (7) is identical to Equation (6) except that the same value of m and b are assumed for each laminate within a slab.

We conducted a test to determine whether the reduced model provided an acceptable fit to the data.³⁰ This test resulted in a statistical F value that was compared with tabled F values on (4, 12) degrees of freedom (Table 1). The tabled 5 percent F value is 3.26. Because calculated F values are less than the tabulated F values, this reduced model is clearly acceptable for five slabs (20, 22, 32, 35, 39), not acceptable for one slab (43), and marginal for two slabs (3, 33). We concluded that overall the reduced model was acceptable for Equation (2). In Table 1, we provide the estimate form and b for each slab along with the estimated standard errors. We also tabulated the statistical coefficient of determination (R^2) for each slab. Note that the R^2 is very high for all slabs, with the reduced model values only marginally smaller than the full-model values.

The second issue to consider was how well the model fit the data. In general, Equation (2) tended to underpredict the time at the 13- and 38-mm depths and overpredict at the 25-mm depth. A comparison of time and char depth for test number 20 illustrates this point (Figure 1). A formal lack-of-fit test was conducted to quantify this potential model misfit. This test resulted in an F value to be compared to tabled F values (3, 9); the 5 percent significance level was 3.86. Four of the slabs (3, 20, 32, 33 in Table 1) were clearly subject to lack of fit, suggesting that Equation (2) is not an adequate description of the data.

We conducted similar analyses on all the equations. The results for Equation (1) were similar to those for Equation (2); the reduced model was acceptable but with excessive lack of fit. For Equation (4), the reduced model was generally not acceptable (the different laminates could not be described by the same equation) but without excessive lack of fit. For Equation (5), the results on the acceptability of the reduced model were somewhat mixed. For some boards, the reduced model was not acceptable. There was no excessive lack of fit for Equation (4). We also noted that the R^2 values obtained from Equations (4) and (5) were somewhat higher than for Equations (1) and (2). We conclude that Equation (4) is the best of the four models we considered. We also view the reduced model form as being acceptable.

Our chosen model, Equation (4) [or Equation (3)], specifies a nonlinear relationship between time and char depth that is described by two parameters. These two parameters are determined separately from the experimental data for each slab. The main disadvantage of Equation (4) is that it has two parameters. In developing an empirical model to predict these

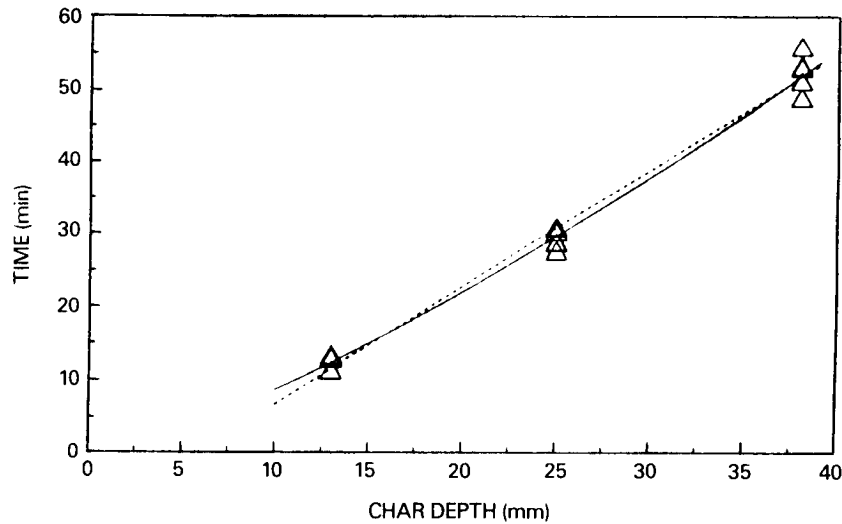


Figure 1: Data for Equation (2) (---) and Equation (3) (—) (Test number 20)

parameters based on the properties of the wood, it would be better if only one parameter in the time-location model needed to be determined.

The possibility of developing a single-parameter model was examined by evaluating Equations (4) and (5) with one of the parameters assumed to be a constant across all slabs. In this case, the "full" model was the model with two parameters for each slab, and the "reduced" model was the model with one parameter that varies from slab to slab and the one parameter that is constant for all slabs. We tested the acceptability of the reduced model using the data from all 40 slabs.

For Equation (4), we tested both the hypothesis that m was constant and the hypothesis that a was constant for all 40 tests. For both tests, the tabulated F value corresponding to 1 percent significance was 1.6. The computed F values were 2.0 (for constant a) and 49,000 (for constant m). Similar tests then were conducted using Equation (5). The computed F values were 2.6 (for constant g) and 4.5 (for constant d). Thus, the null hypothesis, which states that one parameter could be held constant, was rejected in all cases.

However, we conclude that Equation (4) with constant a provided a substantial gain in simplicity and interpretability in subsequent analysis. The computed F value was the smallest for the constant a model. Moreover, in fitting separate models for each slab, we noted that the range of slab-specific estimates of a was very small. The coefficient of variation for those estimates was only 4 percent.

Based on the previous factors, the model of a constant a in Equation (4) was selected as an acceptable single-parameter model. Written in the

original model form of Equation (3), this becomes

$$t = mx_c^{1.23} \quad (8)$$

This model indicates that as charring progresses, the rate of charring decreases slightly. This is consistent with the thicker char layer acting as an insulative layer. For subsequent development of models relating the physical and chemical properties of the wood with the charring rate ($1/m$), we used the logarithmic form of Equation (8). Using the data from all 40 slabs, we estimated slab-specific values for $\ln m$ from the logarithmic form of Equation (8) and form of Equation (8).

Regression of Charring Rates with Properties

We used regression analysis to develop empirical models relating $\ln m$ to the material properties. The charring rate and char contraction factor responses of the 40 charring tests were regressed on property data obtained in the charring tests and the supplementary tests. A detailed discussion of the development of the empirical models for $\ln m$ was given by White.⁷ For this paper, our results are expressed in terms of equations form of Equation (8). We evaluated numerous regression models in arriving at a final model. Initially, the charring rate was assumed to be a function of four factors—density, moisture content, chemical property, and transport property. The goal was to have an equation that can be used to predict the charring rate of different species.

Our methodology consisted of backward, stepwise, and maximum R^2 selection procedures to arrive at candidate models. The most successful models were response surface models including linear, quadratic, and cross product terms in which one independent variable was selected from each of the four groups of factors. Expressed as an equation form, the final model was

$$m = 0.162 + 0.809p + 0.0107u + 0.0689c - 0.00655pd - 0.00240cd \quad (R^2 = 0.764) \quad (9)$$

in which p is oven-dry density or specific gravity, u is percentage moisture content, and c is hardwood-softwood classification. The value for the classification variable was 1 for softwoods and -1 for hardwoods. Variable d , which does not appear as a linear term, is depth of CCA penetration in millimeters; included in the model are the cross-product terms pd , and cd . The root mean square error for Equation (9) is 0.051. The maximum value for d in all equations was 63 mm. The specimens used to determine the depth of CCA penetration (d) were 63 mm deep.

Equation (9) is based on the factorial experimental design of the study. The mean densities for the species representing low and high densities in the factorial experimental design were significantly different (Table 2).

Table 2: Average char rates and properties of species used in the factorial experimental design.^a

Species	Reciprocal of char rate m ^b		Char contraction factor	Klanson lignin (%)	Density ^c (g/cm ³)	Depth of penetration (mm)
	Equation (8) (min/mm ^{1.23})	Equation (1) (min/mm)				
Softwoods						
Engelmann spruce	0.7338 (A)	1.62 (A)	0.835 (A)	27.3	0.425 (C)	3 (C)
Western red cedar	0.5541 (C,D)	1.22 (C,D)	0.784 (B)	33.2	0.310 (E)	3 (C)
Southern pine	0.5547 (C,D)	1.23 (C,D)	0.589 (D)	27.9	0.509 (B)	31 (B)
Redwood	0.5976 (B,C)	1.32 (B,C)	0.862 (A)	37.1	0.343 (D,E)	4 (C)
Hardwoods						
Hard maple	0.6530 (B)	1.44 (B)	0.594 (D)	22.4	0.691 (A)	47 (A)
Yellow poplar	0.6068 (B,C)	1.34 (B,C)	0.672 (C)	21.3	0.504 (B)	5 (C)
Red oak	0.7470 (A)	1.65 (A)	0.703 (C)	24.5	0.664 (A)	3 (C)
Basswood	0.4980 (D)	1.10 (D)	0.542 (D)	19.8	0.399 (C,D)	30 (B)

^aMeans with the same letter are not significantly different based on Duncan's multiple range test.

^bMean of results with different moisture contents.

^cBased on weight and volume oven-dried.

Significant differences were also found in the depths of CCA penetration for the different species. But, the desired factorial design was not completely obtained. Neither of the two low-density softwoods had high treatability. Results for both the red cedar and redwood specimens indicated low transverse treatability. The softwood species had higher Klason lignin contents than did the hardwood species. The mean density of the four hardwood species was significantly higher than the mean density of the four softwood species. The experiments revealed significant differences in the mean charring rates for the different species even though the means were based on data for various moisture content levels (Table 2). Table 2 lists the mean values for the properties that were used in the final models. The results of the supplementary tests are given in more detail by White.⁷

Equation (9) is limited to the materials property data considered in the original experimental design. As shown later, the terms c and cd are also predictors of the char contraction factor. The char contraction factors also appeared to be independent of the moisture content. As an alternative to Equation (9), equations were developed using the char contraction factor as one of the material properties. As before, we examined various combinations of the transport and chemical properties in response surface models. The resultant alternate model is

$$m = -0.147 + 0.564p + 0.0121u + 0.532f_c \quad (R^2 = 0.755) \quad (10)$$

where f_c is the char contraction factor. The root mean square error for Equation (10) is 0.050.

Equations (9) and (10) are consistent with the rate of charring (l/m), decreasing with increasing density or moisture content. Equation (10) also indicates that the rate of charring decreases with increases in the char contraction factor. This is consistent with a thicker char layer providing more of an insulative layer. Equation (10) suggests that c , pd , and cd are variables related to the char contraction factor (Table 3).

A third alternative model for m was developed by assuming a hypothetical species-specific coefficient addition to Equation (10). One main hypothesis of this study was that an equation for charring rate should include a term relating the moisture effect to the permeability of the wood. Consistent with this hypothesis, the impermeable species caused the greatest difficulty with Equation (10). The initial hypothesis, based on work by White and Schaffer,¹⁸ was that charring occurs at a slower rate when the impermeability of the wood prevents the vaporized moisture from being driven into the wood and recondensing. That is, moisture driven into the wood has no net effect on the energy balance within the wood. With respect to Equation (10), the predicted rates were for faster charring than that obtained in the tests of the white oak, Douglas fir, and spruce. Thus, it seemed plausible that species-specific coefficients might be most appropriate for moisture content. Regression analyses allowing for such species-

specific coefficients resulted in

$$m = 0.1526 + 0.5080p + 0.1475f_c + Z_1u \quad (R^2 = 0.906) \quad (11)$$

where values for Z_i are listed in Table 4. The f_c parameter in Equation (11) was not statistically significant. This is likely due to the high correlation between the char contraction factor and the permeability of the wood. The relative ranking of the species was consistent with their permeability (Figure 2). The first three species (pine, maple, and basswood) were the three permeable species and the species with the smallest char contraction factors. The values for Z_i are consistent with our initial hypothesis. The higher Z values of the impermeable species resulted in predictions of slower charring rates.

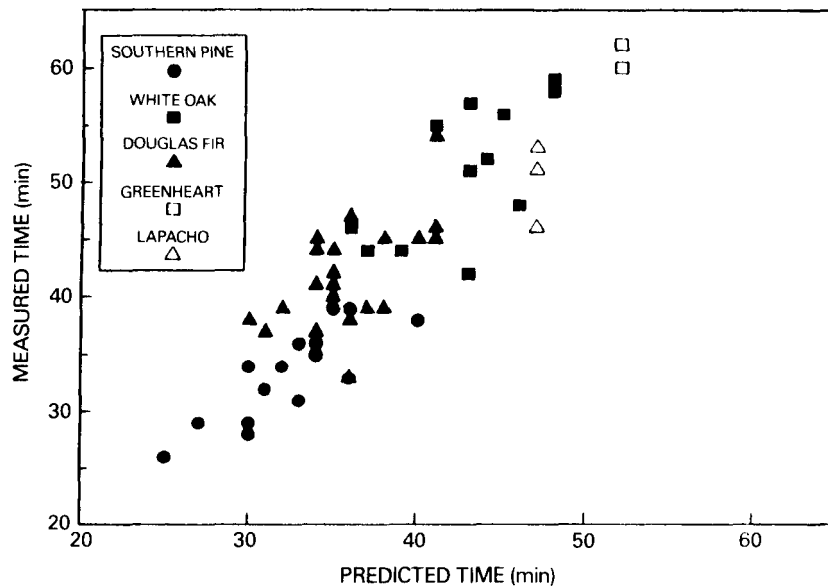


Figure 2: Equation (10) predictions for times for char depths of 25.4 mm with experimental data in the literature.

Regression of Char Contraction Factors With Properties

Significant differences were found in the char contraction factors of the different species (Table 2). To better understand the char contraction factor, we investigated various empirical models for this factor using the same procedure that we used with in m . The resulting equation is

$$f_c = 0.732 - 0.00423d + 0.203c - 0.00164cd - 0.270pc \quad (R^2 = 0.842) \quad (12)$$

We also found a significant relationship ($R^2 = 0.555$) between the char contraction factor and the Klason lignin content. This is consistent with

Table 3: Parameter estimates for Equations (9) and (10) of the response m [Eq. (8)]

Equation	Variable ^a	Parameter estimate	Standard error	R^2	Coefficient of variation
9	Constant	0.16229	0.04687	0.764	8.23
	p	0.80939	0.08724		
	c	0.06886	0.01431		
	u	0.010710	0.002446		
	pd	-0.006551	0.001001		
	cd	-0.0024044	0.0005657		
10	Constant	-0.14691	0.07649	0.755	8.15
	p	0.56374	0.06344		
	u	0.012068	0.002386		
	f_c	0.53157	0.07472		

^a p is oven-dry density or specific gravity; c is hardwood-softwood classification ($c = 1$ for hardwood and 1 for softwood); d is depth of CCA penetration in mm; u is percentage moisture content; f_c is char contraction factor as fractional thickness remaining.

Table 4: Species-specific coefficients (Z_i) for Equation (11)

Species	Z_i
Southern pine	0.0050
Hard maple	0.0063
Basswood	0.0080
Yellow poplar	0.0097
Western red cedar	0.0113
Redwood	0.0156
Red oak	0.0161
Engelmann spruce	0.0205

lignin contributing mainly to char, whereas cellulose and hemicellulose mainly form the pyrolysis gases. The higher f_c for softwoods [$c = + 1$ in Equation (12)] is also consistent with their higher lignin content.

Evaluation and Discussion

Time-Location Models

For general use, the simple linear model [Equation (1)] is a suitable model for charring wood under ASTM E 119 fire exposures. However, we found the exponential model [Equation (3)] or its linear logarithmic equivalent [Equation (4)] provided a better fit of the time-location data for the base of the char layer. Additional evaluation of the time-location data indicated that the model could be simplified to a single parameter. The time-location models were not necessarily valid for depths <13 mm or >38 mm.

Past Forest Products Laboratory (FPL) test data were re-evaluated to determine whether they were consistent with our conclusion of a 1.23 value for the parameter a . These data included 42 tests of Douglas fir, southern pine, and white oak specimens done by Schaffer,¹³ 6 tests of southern pine, white oak, and Douglas fir specimens done by White and Schaffer,¹⁸ and 12 miscellaneous tests of Douglas fir, greenheart (*Ocotea rodiaei*), and lapacho (*Tabebuia* sp.) specimens. Greenheart and lapacho are Latin American hardwoods.

The results of Schaffer¹³ were consistent with a simple model in which a has a value of 1. The 1.09 to 1.35 values for a obtained with the six tests of White and Schaffer¹⁸ were more consistent with the average 1.23 value that we obtained in this study. The results for the 12 miscellaneous tests ranged from 0.90 to 1.24 and averaged 1.06. Plots of residuals for the simple model ($a = 1$) indicated no consistent lack of fit for the previous data.

Lawson and others²⁷ reported a model for Douglas fir floor joists in which the exponent a would be 1.25, which is consistent with our 1.23 estimate. Based on tests of different glued laminated beams, Terming-J' reported char depths of 23 and 35 mm for 30 and 60 rein, respectively. Assuming no differences between the beams, those results indicated an exponent a of 1.64.

One explanation for the nonlinear behavior in the current study is that heat was transferred out the back of the slab at the end of the test and that this heat loss was responsible for the longer times at 38 mm. Past test data indicated that the temperature at 63 mm would be 35°C to 70°C when the temperature at 38 mm was 288°C. Repeating the analysis using only the 13- and 25-mm data resulted in a very slight reduction (1.23 to 1.2) in the exponent a . It is unlikely that a sufficient heat loss occurred at the back side of the 63-mm-thick slab to affect the times for the 288°C criteria at the 25-mm location. A second possibility for the conflict in a is that the fire ex-

posure was different. Although all the FPL tests were run in the same furnace, the arrangement of the burners and the furnace thermocouples was different in the earlier tests of Schaffer.¹³

In addition to possible differences in the heat flux, the amount of ventilation may be a factor. More ventilation may increase char oxidation at the surface. Char oxidation did not seem to be significant in our experiments. Char oxidation is probably more likely in the later part of an ASTM E 119 test when the furnace temperatures are higher. The nonlinear time-location model is consistent with a char layer that is a fixed percentage of the original wood thickness. Charring would be slower as the insulative char layer gets thicker. In the ASTM E 119 test, the continuing increase of furnace temperature reduces the effect of the thicker char layer. Additional surface recession from char oxidation in the latter part of the test would have also increased the charring rate and resulted in a more linear time-location model. Additional testing and computer modeling are needed to determine how the single-parameter time-location model [Equation (8)] is dependent on the test conditions.

Char Contraction Data

The thickness of the charred slab after the test was less than the original thickness of the wood slab. In previous work,²⁴ this surface recession was an important factor in the theoretical modeling of wood charring. In our study, we developed empirical models for the char contraction factor [Equation (12)]. As shown by Equation (12), various factors affected the char contraction.

The hardwood-softwood classification correlated to the contraction of the char layer because it also correlated to the lignin content of the wood. The main differences in chemical composition between the hardwoods and softwoods were the amount of lignin and the types of the hemicelluloses. Higher lignin content levels resulted in a higher fractional residual weight. This higher residual weight was consistent with the predictions of less contraction. Parker³² has shown the char contraction factor to be a function of the mass fraction remaining after degradation. The significance of the treatability on the contraction was less clear. The models suggested that the more treatable woods have greater contraction.

To better understand these data, the char contraction factors in the charring tests (Table 2) were compared with data in the literature. The contraction associated with the charring of dry wood in a nitrogen environment has been reported in the literature.³²⁻³⁵ The char contraction factors were calculated from the contraction ratios of Beall³³ and Evans³⁴ and compared with the contraction factors obtained in the charring tests. The differences between the two sets of contraction factors were consistent with a version of Equation (12) that included annual ring orientation. Char contraction factors for pine and oak in our study agree with data of Parker,³²

White and Schaffer,¹⁸ and Slocum and others.³⁵ Predicted char contraction factors for Douglas fir were in agreement with data of Beall,³³ White and Schaffer¹⁸ and Truax.³⁶

As just discussed, the char contraction factor obtained from the charring tests compared very favorably with literature results for contraction of wood charred in a nitrogen environment. Char oxidation might also have caused surface recession. The agreement of the contraction factors with contraction factors for nitrogen environment suggests that char oxidation was not a major factor in our charring tests. This is consistent with a finding that charring rate was independent of furnace oxygen level (3 to 13 percent).³⁷ The outflow of pyrolysis gases and water vapor from the burning wood slab possibly prevented any oxidation at the surface. Kanury and Blackshear⁸ noted that if a flame envelops the decomposing solid, the diffusion of oxygen into the subsurface layers of wood maybe neglected. The small vertical furnace had natural gas burners and natural ventilation provided by holes near the base of the furnace. In other fire exposures, char oxidation may be an important factor.

Predictive Char Rate Models

The charring rate parameter was significantly different for the various species. Numerous empirical models were considered as predictors of the charring rate. Equations (9) and (10) were selected as the best and most practical equations to predict the charring rate. The char contraction factor (f) in Equation (10) was a significant improvement to the model. A model with just density and moisture content has a R^2 value of only 41.1 percent compared with the 75.5 percent of Equation (10) and a root mean square error of 0.077 compared with 0.050 for Equation (10). Better understanding of the movement of moisture in a charring wood slab may lead to improved predictive models. Equation (10) results suggest that the hardwood-softwood classification and depths of CCA penetrations are correlated to the charring rate because of their correlation to the contraction of the char layer. Models involving additional terms beyond the more basic selected model were developed.⁷ Although the additional factors slightly improved the R^2 value, the addition of some factors maybe due to only small parts of these data and needs to be verified by additional systematic testing.

Equation (9) was based on data obtained using a factorial experimental design and was developed by a systematic selection process based on backward, stepwise, and maximum R^2 value selection procedures. The physical significance of the trends indicated by the models was also considered. There does appear to be physical significance for the various models. This was particularly true with Equation (10) that involved just three main effects—density, moisture content, and char contraction factor.

It should be stressed that empirical models reflect correlations between

the response and the independent variables and not necessarily causality. Other factors must be considered when interpreting the physical significance of the empirical models. The models were selected based on their ability to predict the charring rates. They may not reflect the actual effect that an arbitrary change in an independent variable has on the response or dependent variable. We mention this particularly because Equation (9) had interactions that included the depth of penetration variable even though the depth of penetration was not a main variable. You cannot conclude from this equation that depth of penetration does not have a main effect on the charring rate.

These cautions are important because of correlations between the independent variables. Although one benefit of a factorial design is the orthogonal relationship between the main effects, natural correlations between the properties of wood made a true factorial design nearly impossible. Density has a significant effect on most wood properties. Relationships between the independent variables may not always be obvious. For example, lower lignin content can result in deeper CCA penetration because lignin increases the fixation rate.³⁸ Also, significant correlations were evident between the char contraction factor and several of the other independent variables.

As mentioned, there does appear to be physical significance for the various models. Because charring involves the thermal degradation of wood mass, the charring rate is slower when there is greater mass to degrade. The higher moisture content level means that more heat is absorbed by the vaporization of the moisture and less heat is available to degrade the wood. The char layer is believed to act as an insulative layer over the uncharred wood. The thicker the char layer is for a given char depth, the greater the thermal insulation effect and the slower the charring rate.

As with the time-location model, we applied the predictive char rate model (Equation 10) to the FPL data and the literature results to evaluate its predictive capability. Linear regression analysis was used to evaluate the predictions. In predicting the char contraction factor Equation (12), a depth of CCA penetration of 3 mm was assumed for Douglas fir, white oak, greenheart, and lapacho. A value of 36 mm was assumed for southern pine. Reasonably good agreement was found between the predicted times for 25.4 mm of char and the experimental data (Figure 3). Linear regression of the experimental data with the predicted data as the predictor (zero intercept) resulted in a slope of 1.13 for Equation (10). Very good agreement was found for the southern pine data, but the predictions for Douglas fir and white oak were for faster charring than the experimental data. Although the graphs of the predictions with the experimental data showed some discrepancies with the Douglas fir and white oak data, the model with the

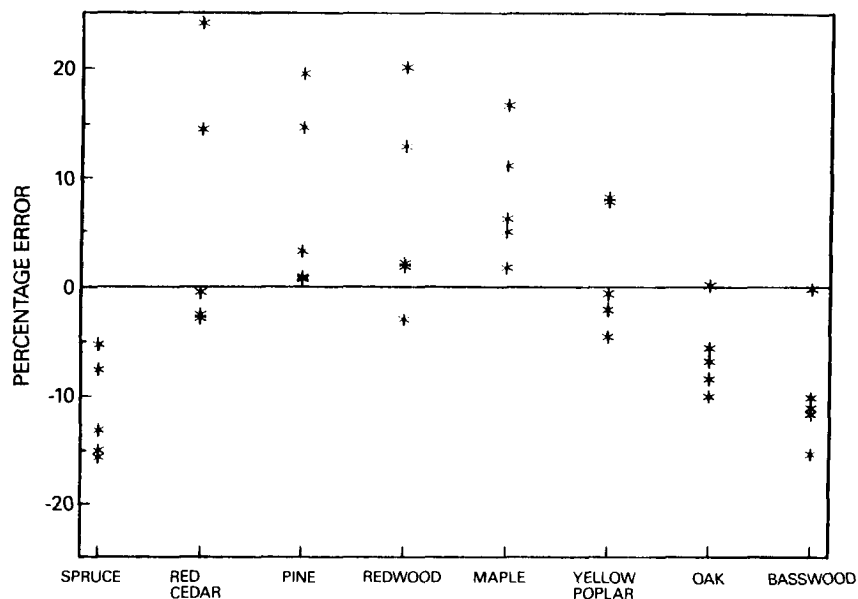


Figure 3: Percentage error in predicting charring rates of one species from models generated using the other seven species. The model for m includes density, moisture content, and char contraction factor.

char contraction factor represented a consequential improvement over the model with just density and moisture content.

To further evaluate the models, we investigated the effect of the individual species on the predictive charring models by repeating the regression analysis without data of one species. The resulting equations were used to predict the data excluded from the analysis. For Equation (10) (Figure 4), all the predicted charring rates for spruce were too fast. Like Douglas fir and white oak, spruce is an impermeable species. All the predicted charring rates for maple, a permeable species, were too slow.

It is clear that Equation (10) with density, moisture content, and char contraction factor did not include all the significant factors affecting the charring rate. In Equation (11), we added a hypothetical species-specific coefficient to Equation (10). Prediction of the literature data with Equation (11) resulted in some improvement over Equation (10). Linear regression of the experimental data with the predicted data as the predictor resulted in a slope of 1.10. The Z_i value of red oak was assumed for white oak, greenheart, and lapecho. The Z_i value of spruce was assumed for Douglas fir. Ideally, we wanted to find an additional factor that could provide comparable information as the species-specific coefficient.

As just discussed, the models tended to predict faster than actual

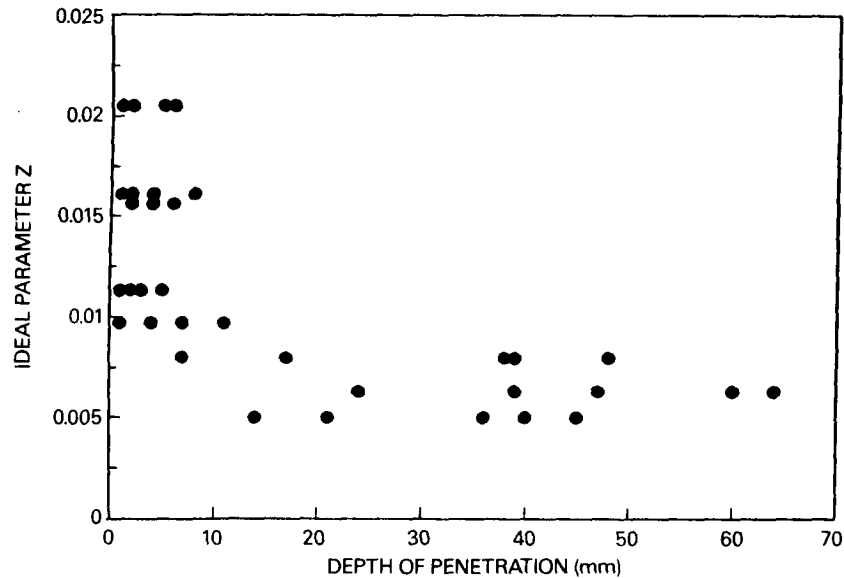


Figure 4: Species-specific coefficients (Z_1) of Equation (11) compared to depth of penetration, and indicator of permeability.

charring rates for a high-density, impermeable species. This may have resulted from other factors affecting the charring rate of the other species. This is likely to be related to movement of moisture within the specimen and its effect on the charring rate. Other possible factors affecting the charring rate may have been nonlinearity in the effect of density, anatomical effects such as ring orientation, and chemical factors such as extractive contents. Additional tests need to be done to clarify these other factors.

Some disagreement between the predicted charring rates and the literature values may have been due to variabilities in the d and f_c values for a given species. For the data of Schaffer,¹³ the regressions for the species-dependent models of density and density times moisture content had R^2 values of only 0.73, 0.49, and 0.58 for Douglas fir, southern pine, and white oak, respectively. This "board effect" was observed in the properties and test results of our study. Differences between two boards of the same species can be greater than the differences between two boards of different species. Also, the question of uniformity of material properties within the wood samples remains.

For this work, the empirical models given by Equations (9) or (10) provide the best and most practical equations to predict the charring rate of different species of wood when exposed to direct ASTM E 119 fire conditions. Equation (11) results suggest the type of parameter that is

needed to improve the predictive capability of the model. It remains likely that the missing parameter is some sort of permeability factor associated with the movement of moisture behind the char front.

Conclusions

Forty charring tests were conducted to develop empirical models [Equations (9) and (10)] to understand the variability in charring rates. We found that a nonlinear time-location model more accurately reflects the location of the base of the char layer (x_c) at a given time than does a simple linear model. Additional testing and computer modeling are needed to determine how the time-location model is dependent on the test conditions.

The charring rate parameter was regressed against various physical and chemical properties. The two most important properties in the charring of wood are density and moisture content. In further development of the models, we determined that the contraction of the wood as it thermally degrades to char was also important. The char contraction factor is mainly related to the lignin content of the wood or the hardwood-softwood classification, because the lignin content of the softwoods is generally greater than that of the hardwoods. Recession of the char surface in these experiments appears to be due to contraction of the char and not due to char oxidation or ablation. Evaluation of the model suggests that all factors affecting the charring rate are not being accounted for by the model. A model was developed [Equation (11)] that should help in identifying missing factors. Although other possible factors include chemical composition, anatomical characteristics, and moisture movement, permeability remains a likely missing factor.

These practical models can be used to predict the charring rate of different wood species when directly exposed to ASTM E 119 fire exposure. The models assume that the thickness of the wood is such that it can be considered a semi-infinite slab. The understanding of the behavior that resulted in these empirical models will aid the development of suitable theoretical models.

ACKNOWLEDGMENT

This study was conducted while the senior author was a graduate student in the Forestry Department of the University of Wisconsin-Madison. Hans Kubler served as his major professor.

Nomenclature

Unless otherwise indicated, the nomenclature is as follows:

a	empirical parameter
b	empirical parameter
c	hardwood (-1) - softwood (+1) classification
d	depth of penetration in treatability test, mm
e	error in estimate, min
f_c	char contraction factor, dimensionless
g	empirical parameter
m	reciprocal of charring rate as defined by Equation (8), min/mm
p	density from oven-dry mass and volume, g/cm ³
R	correlation coefficient, dimensionless
t	time, min
u	moisture content, percent
x_c	char depth from original fire-exposed surface, mm
Z_1	empirical parameter with coefficient of 1 in Equation (11)

References

1. "Standard Methods of Fire Tests of Building Construction and Materials." Designation E 119-83, American Society for Testing and Materials, Philadelphia, PA, 1983.
2. White, Robert H., "Analytical Methods for Determining Fire Resistance of Timber Members." In: *SFPE Handbook of Fire Protection Engineering*, National Fire Protection Association, Quincy, MA, 1988.
3. Atreya, Arvind, "Pyrolysis, Ignition and Flame Spread on Horizontal Surfaces of Wood." Ph.D. diss., Harvard University, Cambridge, MA, 1983.
4. Fredlund, Bertil, "A Model for Heat and Mass Transfer in Timber Structures during Fires." Institute of Science and Technology, Department of Fire Safety Engineering, Lund University, Lund, Sweden, Report LUTVDG/(TV BB.1003), 1988.
5. Hadvig, Sven, "Charring of Wood in Building Fires." Laboratory of Heating and Air-Conditioning, Technical University of Denmark, Lyngby, Denmark, 1981.
6. Parker, William J., "Prediction of the Heat Release Rate of Wood." Ph.D. diss., George Washington University, Washington, DC, 1988.
7. White, Robert Hawthorne, "Charring Rates of Different Wood Species." Ph.D. diss., University of Wisconsin, Madison, WI, 1988.
8. Kanury, Murty A. and Blackshear, Perry L. Jr., "Some Considerations Pertaining to the Problem of Wood-Burning." *Combustion Science and Technology*, 1 (1970): 339-356.
9. Lee, Calvin K., Chaiken, Robert F., and Singer, Joseph M., "Charring in Pyrolysis of Wood in Fires by Laser Simulation." In: *Sixteenth*

- Symposium (Int.) on Combustion*, pp. 1459-1470, The Combustion Institute, Pittsburgh, PA, 1977.
10. Bryan, J., and Doman, J.S., "Fire Resistance - The Comparative Resistance to Fire of Various Species of Timber." *Wood*, 5 (1940): 19-23.
 11. McNaughton, G.C., "Comparative Performance of Different Species of Untreated Wood in Various Fire-Test Methods." U.S. Department of Agriculture, Forest Service, Forest Products Laboratory, Madison, WI, 1942.
 12. Thomas, P.H., and Simms, D.L., and Law, Margaret, "The Rate of Burning of Wood." Fire Research Note No. 657, Fire Research Station, Borehamwood, England, 1967.
 13. Schaffer, E.L., "Charring Rate of Selected Woods—Transverse to Grain." Research Paper FPL 69, U.S. Department of Agriculture, Forest Products Laboratory, Madison, WI, 1967.
 14. Rogowski, Barbara, "Charring of Timber in Fire Tests." In: *Fire and Structural Use of Timber in Buildings*, Fire Research Station Symposium No. 3, London: HMSO, 1970.
 15. Hall, G.S., Saunders, R.G., Allcorn, R.T., Jackman, P.E., Hickey, M.W., and Fitt, R., "Fire Performance of Timber—A Literature Survey." Timber Research and Development Association, High Wycombe, England, 1972.
 16. Williams, C.C., "Damage Initiation in Organic Materials Exposed to High Intensity Thermal Radiation." Ph.D. diss., Massachusetts Institute of Technology, Cambridge, MA, 1953.
 17. Dorn, H., and Egner, K., "Fire Tests on Glued Laminated Structural Timbers (Glulam Beams)." Translated by D.A. Sinclair. Technical Translation No. 1131, Ottawa: National Research Council of Canada. Trans. of "Brandversuche mit geleimten Holzbauteilen (Hetzer-Balken)," *Holz-Zentralblatt*, 28 (1964): 435-438.
 18. White, Robert H., and Schaffer, E.L., "Transient Moisture Gradient in Fire-Exposed Wood Slab." *Wood and Fiber*, 13 (1981): 17-38.
 19. Tinney, E. Roy, "The Combustion of Wooden Dowels in Heated Air." In: *Tenth Symposium (Int.) on Combustion*, 925-930, The Combustion Institute, Pittsburgh, PA, 1965.
 20. Roberts, A.F., "A Review of Kinetics Data for the Pyrolysis of Wood and Related Substances." *Combustion and Flame*, 14 (1970): 261-272.
 21. Tang, W.K., "Forest Products." In: *Differential Thermal Analysis*, edited by R.C. Mackenzie, Vol. 2 Applications, 523-553. Academic Press, New York, NY, 1972.
 22. Knudson, R.M., and Williamson, R.B., "Influence of Temperature and Time Upon Pyrolysis of Untreated and Fire Retardant Treated Wood." *Wood Science and Technology*, 5 (1971): 176-189.

23. Hadvig, Sven, and Paulsen, O.R., "One-Dimensional Charring Rates in Wood." *J. Fire and Flammability*, 7 (1976): 433-449.
24. White, Robert H., and Schaffer, E.L., "Application of CMA Program to Wood Charring." *Fire Technology*, 14 (1978): 279-290, 296.
25. Roberts, A.F., "The Heat of Reaction During the Pyrolysis of Wood." *Combustion and Flame*, 17 (1971): 79-86.
26. Snedecor, George W., and Cochran, William G., *Statistical Methods*, 7th ed, The Iowa State University Press, Ames, IA, 1980.
27. Lawson, D.E., Webster, C.T., and Ashton, L.A., "The Fire Endurance of Timber Beams and Floors." *Structural Engineer*, 30 (1952): 27-33.
28. Vorreiter, Leopold., "Combustion and Heat Insulating Losses of Wood and Fiber Boards." Translated by Research Information Service, Translation No. 321, Madison, WI: U.S. Department of Agriculture, Forest Service, Forest Products Laboratory. Trans. of "Abbrandverlust und Temperaturdämmung von Holz und Holzwerkstoffen," *Holzforschung*, 10 (1956): 75-80.
29. Kanury, Murty A., and Holve, Donald J., "A Theoretical Analysis of the ASTM E 119 Standard Fire Test of Building Construction and Materials." National Bureau of Standards, Washington, DC, NBS-GCR 76-50, 1975.
30. Draper, N.R. and Smith, H., *Applied Regression Analysis*, 2nd ed. New York, NY, John Wiley & Sons, 1981.
31. Tenning, K., "Glued Laminated Timber Beams: Fire Tests and Experience in Practice." In: *Fire and Structural Use of Timber in Buildings*, Symposium No. 3, Fire Research Station, London: HMSO, 1970.
32. Parker, William J., "Development of a Model for the Heat Release Rate of Wood—A Status Report." National Bureau of Standards, Gaithersburg, MD, Report NBSIR 85-3163, 1985.
33. Beall, F.C., "Properties of Wood During Carbonization Under Fire Conditions." In: *Wood Technology: Chemical Aspects*, edited by Irving S. Goldstein, Washington, DC: American Chemical Society, 1977.
34. Evans, D.D., "Density of Wood Charcoal." Cambridge, MA: Harvard University, Home Fire Project Technical Report No. 14, 1975.
35. Slocum, D.H., McGinnes, E.A, Jr., and Beall, F.C., "Charcoal Yield, Shrinkage, and Density Changes During Carbonization of Oak and Hickory Woods." *Wood Science*, 11, (1978): 42-47.
36. Truax, T. R., "Fire Research and Results at the Forest Products Laboratory." Report No. 1999, U.S. Department of Agriculture, Forest Service, Forest Products Laboratory, Madison, WI, 1959.
37. Malhotra, H.L., "Design of Fire-Resisting Structures." Chapman and Hall (Surrey University Press), New York, NY, 1982.
38. Jansen, A., Pizzi, A., and Conradie, W.E., "The Penetration Characteristics of CCA Preservatives in Wood-Radial/Tangential, Processes and Species Effects." *Holz als Roh- und Werkstoff*, 43, (1985): 181-186.